2013 IEEE/RSJ International Conference on
Intelligent Robots and Systems (IROS)
November 3-7, 2013. Tokyo, Japan

Control of Bilateral Teleoperators in the Operational Space without Velocity Measurements

Carlos I. Aldana, Emmanuel Nuño and Luis Basañez

Abstract— **This paper proposes a proportional plus damping injection (P + d) controller for bilateral teleoperators in the operational space. Unit quaternions are used to describe the end-effectors' orientation since they exhibit the well known property of being a singularity-free representation. The proposed controller does not need the measurement of the velocities, instead a passivity–based filter is used. Under the reasonable assumptions that the human operator and the environment define passive maps from force to velocity, it is proved that velocities and pose (position and orientation) errors between the local and the remote manipulators are bounded. Moreover, in the case that the human and the environment forces are zero, the velocities and pose errors converge asymptotically to zero. Finally, experimental validation using two robots of 6-Degrees-of-Freedom (DoF) shows the effectiveness of the proposed control scheme.**

I. INTRODUCTION

Bilateral teleoperation enables human operators to execute tasks in remote environments, e.g., nuclear plants, outer space missions, surgery, etc. It allows operators to feel, through the local manipulator, the interaction of the remote manipulator with the environment. Many control schemes have been proposed for bilateral teleoperators in the last years, an insightful historical survey about this line can be consulted in [1] and a control tutorial in [2]. Most of the previous schemes require the knowledge of velocity measurements in their control laws ([3], [4], [5], [6], [7]). Few remarkable exceptions are [8] where a model dependent sliding scheme is used to control a linearized version of the local and remote manipulators, and [9] where the boundedness of the position error is proved using a high gain velocity observer. All these previous works have been developed in the joint space.

The interest of the operational space control, in bilateral teleoperators, becomes evident when the robot manipulators are not kinematically similar (heterogeneous) or when a common task is teleoperated through a cooperative system [10], [11], [12], [13]. Most of these controllers commonly employ the Euler angles to represent the orientation, however they have the well–known problem of the singularity points. The unit quaternions are a singularity-free orientation representation and they have been widely used in different robotics applications ([14], [15], [16], [17], [18]). An interesting survey of unit quaternions for robot control and a demonstration of their advantages over the Euler angles is reported in [19].

This paper presents an extension to the operational space of the controller reported in [20] that has been previously presented in the joint space for kinematically similar manipulators. Compared to the previous work, the present scheme can be used with heterogenous local and remote manipulators, moreover, the unit quaternions are employed to represent the orientation of the end–effectors and thus such representation is singularity-free. The proposed scheme is a proportional plus damping injection (P + d) controller that uses a simple first-order filter that requires only the pose (position and orientation) measurements of the end-effectors, saving the need to use the generally costly and noisy velocity sensors. It is demonstrated that, under the common assumption that the human operator and the environment define passive maps from velocity to force, the controller ensures that velocities and pose errors between the local and remote robot manipulators are bounded. Further, if the human operator and the environment do not exert any forces, it is proved that the velocities and the pose errors asymptotically converge to zero.

The layout of the paper is as follows. In Section II, the operational space dynamic model of the teleoperation system is derived and the unit quaternion kinematics is presented. In Section III is detailed the main result, the P + d controller with proper stability proofs. Experimental validation, using two robot manipulator of 6-DoF, and the conclusions are given in Sections IV and V, respectively.

Notation. $\mathbb{R} := (-\infty, \infty)$, $\mathbb{R}_{>0} := (0, \infty)$, $\mathbb{R}_{\geq 0} := [0, \infty)$. $\lambda_m\{\mathbf{A}\}$ and $\lambda_M\{\mathbf{A}\}$ represent the minimum and maximum eigenvalues of matrix $\mathbf{A}$, respectively. $||\mathbf{A}||$ denotes the matrix-induced 2-norm. $|\mathbf{x}|$ stands for the standard Euclidean norm of vector $\mathbf{x}$. $\mathbf{I}_k$ and $\mathbf{0}_k$ represent the Identity and all-zeros matrices of size $k \times k$. For a given matrix $\mathbf{A} \in \mathbb{R}^{a \times b}$, where $b \geq a$, $\mathbf{A}^\dagger$ is its pseudo-inverse $\mathbf{A}^\dagger := \mathbf{A}^\top(\mathbf{A}\mathbf{A}^\top)^{-1}$. For any function $\mathbf{f} : \mathbb{R}_{\geq 0} \to \mathbb{R}^n$, the $\mathcal{L}_\infty$-norm is defined as $\|\mathbf{f}\|_\infty := \underset{t\geq 0}{sup}|\mathbf{f}(t)|$, $\mathcal{L}_2$-norm as $\|\mathbf{f}\|_2 := (\int_0^\infty |\mathbf{f}(t)|^2 dt)^{1/2}$. The $\mathcal{L}_\infty$ and $\mathcal{L}_2$ spaces are defined as the sets $\{\mathbf{f} : \mathbb{R}_{\geq 0} \to \mathbb{R}^n : \|\mathbf{f}\|_\infty < \infty\}$ and $\{\mathbf{f} : \mathbb{R}_{\geq 0} \to \mathbb{R}^n : \|\mathbf{f}\|_2 < \infty\}$, respectively.

II. TELEOPERATOR DYNAMICS AND KINEMATICS

The local and remote manipulators are modeled as a pair of n_i-DoF fully actuated, revolute joints, manipulators. Their Euler-Lagrange (EL) equations of motion, in joint space, are given by

$$\begin{aligned}\bar{\mathbf{M}}_\ell(\mathbf{q}_\ell)\ddot{\mathbf{q}}_\ell + \bar{\mathbf{C}}_\ell(\mathbf{q}_\ell, \dot{\mathbf{q}}_\ell)\dot{\mathbf{q}}_\ell + \bar{\mathbf{g}}_\ell(\mathbf{q}_\ell) &= \boldsymbol{\tau}_h - \boldsymbol{\tau}_\ell \qquad (1)\\ \bar{\mathbf{M}}_r(\mathbf{q}_r)\ddot{\mathbf{q}}_r + \bar{\mathbf{C}}_r(\mathbf{q}_r, \dot{\mathbf{q}}_r)\dot{\mathbf{q}}_r + \bar{\mathbf{g}}_r(\mathbf{q}_r) &= \boldsymbol{\tau}_r - \boldsymbol{\tau}_e,\end{aligned}$$

where $\mathbf{q}_i, \dot{\mathbf{q}}_i, \ddot{\mathbf{q}}_i \in \mathbb{R}^{n_i}$, $i \in \{\ell, r\}$, are the joint positions, velocities and accelerations, respectively; $\bar{\mathbf{M}}_i(\mathbf{q}_i) \in \mathbb{R}^{n_i \times n_i}$ are the symmetric positive definite inertia matrices;

$\bar{\mathbf{C}}_i(\mathbf{q}_i, \dot{\mathbf{q}}_i) \in \mathbb{R}^{n_i \times n_i}$ are the Coriolis and centrifugal effects matrices; $\bar{\mathbf{g}}_i(\mathbf{q}_i) \in \mathbb{R}^{n_i}$ are the gravitational torques vectors; $\boldsymbol{\tau}_i \in \mathbb{R}^{n_i}$ are the controllers and $\boldsymbol{\tau}_h, \boldsymbol{\tau}_e \in \mathbb{R}^{n_i}$ are the joint torques induced by the human and environment forces, $\mathbf{u}_h$ and $\mathbf{u}_e$, applied at the end-effector of the local and remote manipulator, respectively.

A. Operational Space Dynamics

The pose of the i-end-effector, $i \in \{\ell, r\}$, relative to the world reference frame, is denoted by $\mathbf{p}_i \in \mathbb{R}^3$, for the position, and by $\boldsymbol{\xi}_i \in S^3$, for the orientation that is described by a unit quaternion. The relation between the joint velocities and the end-effector linear $\mathbf{v}_i$ and angular $\boldsymbol{\omega}_i$ velocities, expressed also relative to the world reference frames, is given by

$$\dot{\mathbf{x}}_i = \begin{bmatrix} \mathbf{v}_i \\ \boldsymbol{\omega}_i \end{bmatrix} = \mathbf{J}_i(\mathbf{q}_i)\dot{\mathbf{q}}_i \tag{2}$$

where $\dot{\mathbf{x}}_i \in \mathbb{R}^6$ and $\mathbf{J}_i(\mathbf{q}_i) \in \mathbb{R}^{6 \times n_i}$ is the *geometric Jacobian* matrix. Note that $\mathbf{v}_i = \frac{d}{dt}\mathbf{p}_i = \dot{\mathbf{p}}_i$. Using the principle of the virtual work, the following relations between joint torques and Cartesian forces are obtained

$$\boldsymbol{\tau}_i = \mathbf{J}_i^\top(\mathbf{q}_i)\mathbf{u}_i, \quad \boldsymbol{\tau}_h = \mathbf{J}_\ell^\top(\mathbf{q}_\ell)\mathbf{u}_h,\ \boldsymbol{\tau}_e = \mathbf{J}_r^\top(\mathbf{q}_r)\mathbf{u}_e \tag{3}$$

where $\mathbf{u}_i, \mathbf{u}_h, \mathbf{u}_e \in \mathbb{R}^6$ and $\mathbf{u}_i := [\mathbf{f}_i^\top\ \mathbf{m}_i^\top]^\top$ where $\mathbf{f}_i, \mathbf{m}_i \in \mathbb{R}^3$ represent the linear forces and moments, respectively (similarly, $\mathbf{u}_h, \mathbf{u}_e$ contain the corresponding linear forces and moments). Using the pseudo-inverse of $\mathbf{J}_i(\mathbf{q}_i)$ and (2), yields

$$\ddot{\mathbf{q}}_i = \mathbf{J}_i^\dagger(\mathbf{q}_i)\ddot{\mathbf{x}}_i + \dot{\mathbf{J}}_i^\dagger(\mathbf{q}_i)\dot{\mathbf{x}}_i \tag{4}$$

The dynamical model of the teleoperator in the operational space is

$$\begin{aligned} \mathbf{M}_\ell(\mathbf{q}_\ell)\ddot{\mathbf{x}}_\ell + \mathbf{C}_\ell(\mathbf{q}_\ell, \dot{\mathbf{q}}_\ell)\dot{\mathbf{x}}_\ell + \mathbf{g}_\ell(\mathbf{q}_\ell) &= \mathbf{u}_h - \mathbf{u}_\ell \\ \mathbf{M}_r(\mathbf{q}_r)\ddot{\mathbf{x}}_r + \mathbf{C}_r(\mathbf{q}_r, \dot{\mathbf{q}}_r)\dot{\mathbf{x}}_r + \mathbf{g}_r(\mathbf{q}_r) &= \mathbf{u}_r - \mathbf{u}_e \end{aligned} \tag{5}$$

where (3) and (4) have been substituted in (1) and

$$\mathbf{M}_i(\mathbf{q}_i) := \left(\mathbf{J}_i^\dagger\right)^\top \bar{\mathbf{M}}_i(\mathbf{q}_i)\mathbf{J}_i^\dagger, \quad \mathbf{g}_i(\mathbf{q}_i) := \left(\mathbf{J}_i^\dagger\right)^\top \bar{\mathbf{g}}_i(\mathbf{q}_i),$$
$$\mathbf{C}_i(\mathbf{q}_i, \dot{\mathbf{q}}_i) := \left(\mathbf{J}_i^\dagger\right)^\top \left(\bar{\mathbf{M}}_i(\mathbf{q}_i)\dot{\mathbf{J}}_i^\dagger + \bar{\mathbf{C}}_i(\mathbf{q}_i, \dot{\mathbf{q}}_i)\mathbf{J}_i^\dagger\right).$$

The coordinate frames are defined as follows: $\boldsymbol{\Sigma}_\ell$ is located at the end-effector of the local manipulator and it is referenced to the local world frame $\boldsymbol{\Sigma}_{W,\ell}$; $\boldsymbol{\Sigma}_{W,r}$ is the world reference frame for the remote site and it is assumed that both $\boldsymbol{\Sigma}_{W,\ell}$ and $\boldsymbol{\Sigma}_{W,r}$ have the same orientation and appropriate scaling; $\boldsymbol{\Sigma}_r$ is the frame attached to the remote manipulator end-effector. The teleoperation system elements and its associated coordinate frames are shown in Fig. 1.

The operational space models (5) have the following properties [21], [22]:

P1. $\forall \mathbf{q}_i,\ 0 < \lambda_m\{\mathbf{M}_i\}\mathbf{I}_6 \leq \mathbf{M}_i(\mathbf{q}_i) \leq \lambda_M\{\mathbf{M}_i\}\mathbf{I}_6 < \infty$.
P2. $\forall \mathbf{x} \in \mathbb{R}^6$, $\mathbf{x}^\top(\dot{\mathbf{M}}_i - 2\mathbf{C}_i)\mathbf{x} = 0$.
P3. $\forall \mathbf{x}, \mathbf{y} \in \mathbb{R}^6$, $\exists k_c \in \mathbb{R}_{>0}$, $|\mathbf{C}_i(\mathbf{x}, \mathbf{y})\mathbf{y}| \leq k_c|\mathbf{y}|^2$.
P4. If $\mathbf{y}, \dot{\mathbf{y}}_i \in \mathcal{L}_\infty$ then $\frac{d}{dt}\mathbf{C}_i(\mathbf{x}, \mathbf{y})$ is a bounded operator.

With regards to the human and the environment interactions, this paper makes the following standard assumption:

A1. The human operator and the environment define passive, velocity to force, maps, that is, $\forall t \geq 0$,

$$-\int_0^t \dot{\mathbf{x}}_\ell^\top(\sigma)\mathbf{u}_h(\sigma)d\sigma \geq 0, \quad \int_0^t \dot{\mathbf{x}}_r^\top(\sigma)\mathbf{u}_e(\sigma)d\sigma \geq 0. \tag{6}$$

When the human and environment passivity assumption is not met, Input-to-State Stability can be proved using similar arguments as those in the proof of our main result. This fact is omitted for brevity.

B. Representing the Orientation

The unit quaternions or Euler parameters ($\boldsymbol{\xi} = [\eta\ \ \boldsymbol{\beta}^\top]^\top \in S^3$, $\eta \in \mathbb{R}$ and $\boldsymbol{\beta} \in \mathbb{R}^3$) are a nonsingular orientation representation subject to a unit norm constraint ($\eta^2 + \boldsymbol{\beta}^\top\boldsymbol{\beta} = 1$). This representation can be derived from the rotation matrix ($\mathbf{R} \in SO(3) := \{\mathbf{R} \in \mathbb{R}^{3\times3} : \mathbf{R}^\top\mathbf{R} = \mathbf{I}_3, \det(\mathbf{R}) = 1\}$) which is obtained from the direct kinematics of the robot manipulator [21]. A list of properties and operations with quaternions can be found in [23], [24].

The orientation disparity (error) between two frames, $\boldsymbol{\Sigma}_i$ and $\boldsymbol{\Sigma}_j$, relative to the world frame, can be described by the rotation matrix $\tilde{\mathbf{R}}_{ij} := \mathbf{R}_i\mathbf{R}_j^\top \in SO(3)$. The unit quaternion, $\tilde{\boldsymbol{\xi}}_{ij}$, describing the orientation disparity between these two frames is given by [15], [16], [25]

$$\tilde{\boldsymbol{\xi}}_{ij} = \boldsymbol{\xi}_i \otimes \boldsymbol{\xi}_j^* = \begin{bmatrix} \tilde{\eta}_{ij} \\ \tilde{\boldsymbol{\beta}}_{ij} \end{bmatrix} = \begin{bmatrix} \eta_i\eta_j + \boldsymbol{\beta}_i^\top\boldsymbol{\beta}_j \\ \eta_j\boldsymbol{\beta}_i - \eta_i\boldsymbol{\beta}_j - \mathbf{S}(\boldsymbol{\beta}_i)\boldsymbol{\beta}_j \end{bmatrix} \tag{7}$$

where $\otimes$ denotes the quaternion product; $\boldsymbol{\xi}^* = [\eta\ \ -\boldsymbol{\beta}^\top]^\top$ is the quaternion conjugate and $\mathbf{S}(\cdot)$ is the skew-symmetric matrix operator such that, for all $\mathbf{a} \in \mathbb{R}^3$,

$$\mathbf{S}(\mathbf{a}) = \begin{bmatrix} 0 & -a_3 & a_2 \\ a_3 & 0 & -a_1 \\ -a_2 & a_1 & 0 \end{bmatrix}$$

It is well–known that, for all $\mathbf{a}, \mathbf{b} \in \mathbb{R}^3$, the skew–symmetric matrix operator satisfies:

$$\begin{aligned} \mathbf{S}(\mathbf{a})^\mathrm{T} &= \mathbf{S}(-\mathbf{a}) = -\mathbf{S}(\mathbf{a}) \\ \mathbf{S}(\mathbf{a})\mathbf{b} &= \mathbf{a} \times \mathbf{b} \\ \mathbf{S}(\mathbf{a})\mathbf{a} &= 0. \end{aligned}$$

The relation between the time–derivative of the unit quaternion and the angular velocity, relative to the world reference frame, is given by

$$\dot{\boldsymbol{\xi}}_i = \begin{bmatrix} \dot{\eta}_i \\ \dot{\boldsymbol{\beta}}_i \end{bmatrix} = \frac{1}{2}\mathbf{U}(\boldsymbol{\xi}_i)\boldsymbol{\omega}_i \tag{8}$$

where $\mathbf{U}(\boldsymbol{\xi}_i) \in \mathbb{R}^{4\times3}$ is defined as

$$\mathbf{U}(\boldsymbol{\xi}_i) = \begin{bmatrix} -\boldsymbol{\beta}_i^\top \\ \eta_i\mathbf{I}_3 - \mathbf{S}(\boldsymbol{\beta}_i) \end{bmatrix}$$

Finally, it also holds that

$$\begin{aligned} \dot{\tilde{\boldsymbol{\xi}}}_{ij} = \begin{bmatrix} \dot{\tilde{\eta}}_{ij} \\ \dot{\tilde{\boldsymbol{\beta}}}_{ij} \end{bmatrix} &= \frac{1}{2}\begin{bmatrix} -\tilde{\boldsymbol{\beta}}_{ij}^\top \\ \tilde{\eta}_{ij}\mathbf{I}_3 + \mathbf{S}(\tilde{\boldsymbol{\beta}}_{ij}) \end{bmatrix}\tilde{\boldsymbol{\omega}}_{ij} \\ &\quad - \begin{bmatrix} 0 \\ \mathbf{S}(\tilde{\boldsymbol{\beta}}_{ij}) \end{bmatrix}\boldsymbol{\omega}_i. \end{aligned} \tag{9}$$

where $\tilde{\boldsymbol{\omega}}_{ij} = \boldsymbol{\omega}_i - \boldsymbol{\omega}_j$.

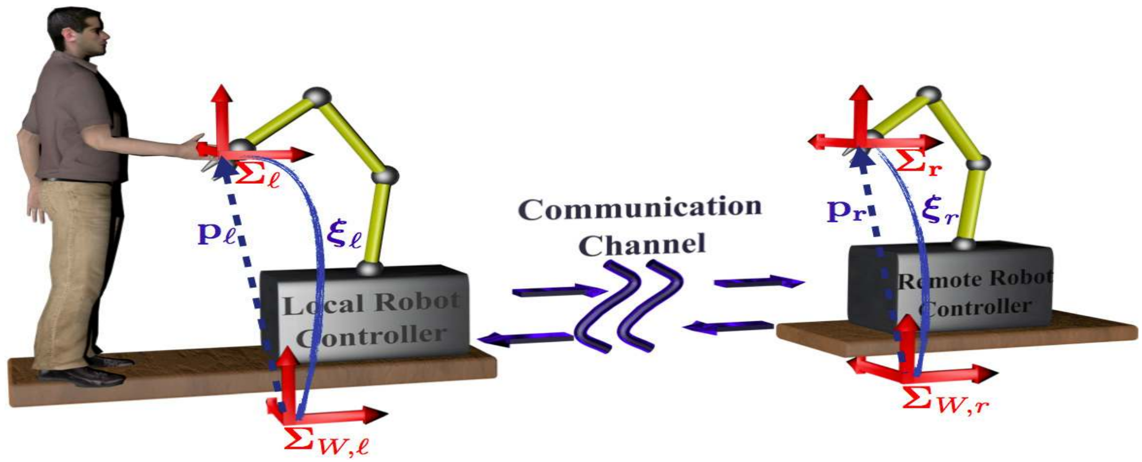

Fig. 1: Elements and coordinate frames of the teleoperation system.

III. Proposed Controllers

Before going through the local and remote proposed controllers, let first us define the following pose error signals, for $i, j \in \{\ell, r\}$ and $i \neq j$

$$\mathbf{e}_{ij} = \begin{bmatrix} \tilde{\mathbf{p}}_{ij} \\ \tilde{\boldsymbol{\beta}}_{ij} \end{bmatrix} = \begin{bmatrix} \mathbf{p}_i - \mathbf{p}_j \\ \eta_j \boldsymbol{\beta}_i - \eta_i \boldsymbol{\beta}_j - \mathbf{S}(\boldsymbol{\beta}_i)\boldsymbol{\beta}_j \end{bmatrix} \tag{10}$$

It should be underscored that $\mathbf{e}_{ij} = \mathbf{0}$ clearly implies that $\mathbf{p}_i = \mathbf{p}_j$. However, it is not trivial to see that it also implies that both orientations are the same. For that reason, we follow the same procedure as in Proposition 1 in [14]. Note that $\mathbf{e}_{ij} = \mathbf{0}$ implies that $\tilde{\boldsymbol{\beta}}_{ij} = \mathbf{0}$ and hence

$$\eta_j \boldsymbol{\beta}_i - \eta_i \boldsymbol{\beta}_j = \mathbf{S}(\boldsymbol{\beta}_i)\boldsymbol{\beta}_j$$

Since $(\eta_j \boldsymbol{\beta}_i - \eta_i \boldsymbol{\beta}_j)$ and $\mathbf{S}(\boldsymbol{\beta}_i)\boldsymbol{\beta}_j$ are orthogonal to each other, the above equation only holds if $\boldsymbol{\beta}_i$ and $\boldsymbol{\beta}_j$ are parallel, hence $\mathbf{S}(\boldsymbol{\beta}_i)\boldsymbol{\beta}_j = \mathbf{0}$. Thus $\boldsymbol{\beta}_i = \frac{\eta_i}{\eta_j}\boldsymbol{\beta}_j$.

On the other hand $\tilde{\boldsymbol{\beta}}_{ij} = \mathbf{0}$ implies that $\tilde{\eta}_{ij} = \eta_i \eta_j + \boldsymbol{\beta}_i^\top \boldsymbol{\beta}_j = \pm 1$ (from the normality condition of the quaternions). Finally

$$\eta_i \eta_j + \frac{\eta_i}{\eta_j} |\boldsymbol{\beta}_j|^2 = \pm 1$$
$$\eta_i(\eta_j^2 + |\boldsymbol{\beta}_j|^2) = \pm \eta_j,$$

hence $\eta_i = \pm \eta_j$, which in turn implies that $\boldsymbol{\beta}_i = \pm \boldsymbol{\beta}_j$. This corresponds to the same orientation in $SE(3)$.

Since in this paper it is assumed that only the local and remote pose is available for measurements, the controllers make use of the following linear velocity estimator

$$\dot{\mathbf{y}}_i = \begin{bmatrix} \dot{\mathbf{y}}_{vi} \\ \dot{\mathbf{y}}_{\omega i} \end{bmatrix} = -\boldsymbol{\Lambda}_i \mathbf{y}_i + \begin{bmatrix} \mathbf{p}_i \\ \boldsymbol{\xi}_i \end{bmatrix} \tag{11}$$

where $\mathbf{y}_i \in \mathbb{R}^7$ is the filter state which is decomposed in two elements $\mathbf{y}_{vi} \in \mathbb{R}^3$ and $\mathbf{y}_{\omega i} \in \mathbb{R}^4$. Matrix $\boldsymbol{\Lambda}_i \in \mathbb{R}^{7\times 7}$ is diagonal and positive definite.

The proposed local and remote controllers are given by

$$\begin{aligned} \mathbf{u}_\ell &= k_\ell \mathbf{e}_{\ell r} + d_\ell \boldsymbol{\Psi}_\ell \dot{\mathbf{y}}_\ell - \mathbf{g}_\ell(\mathbf{q}_\ell) \\ \mathbf{u}_r &= -k_r \mathbf{e}_{r\ell} - d_r \boldsymbol{\Psi}_r \dot{\mathbf{y}}_r + \mathbf{g}_r(\mathbf{q}_r) \end{aligned} \tag{12}$$

where $k_i, d_i \in \mathbb{R}_{>0}$ and

$$\boldsymbol{\Psi}_i = \begin{bmatrix} \mathbf{I}_3 & \mathbf{0}_{3\times 4} \\ \mathbf{0}_3 & \frac{1}{2}\mathbf{U}^\top(\boldsymbol{\xi}_i) \end{bmatrix} \tag{13}$$

The local and remote dynamics (5) in closed–loop with the controllers (12) are

$$\begin{aligned} \mathbf{M}_\ell(\mathbf{q}_\ell)\ddot{\mathbf{x}}_\ell + \mathbf{C}_\ell(\mathbf{q}_\ell, \dot{\mathbf{q}}_\ell)\dot{\mathbf{x}}_\ell + k_\ell \mathbf{e}_{\ell r} + d_\ell \boldsymbol{\Psi}_\ell \dot{\mathbf{y}}_\ell &= \mathbf{u}_h \\ \mathbf{M}_r(\mathbf{q}_r)\ddot{\mathbf{x}}_r + \mathbf{C}_r(\mathbf{q}_r, \dot{\mathbf{q}}_r)\dot{\mathbf{x}}_r + k_r \mathbf{e}_{r\ell} + d_r \boldsymbol{\Psi}_r \dot{\mathbf{y}}_r &= -\mathbf{u}_e \end{aligned} \tag{14}$$

The main result of this paper is the following:

Proposition 1: Consider the bilateral teleoperator (5) and assume that the linear and the angular velocities are not measured. Additionally suppose that Assumption A1 holds. Then, controller (12) with (11) ensure that velocities and pose errors are bounded. Further, if the human operator does not inject forces on the local manipulator and the remote manipulator does not interact with the environment, i.e., $\mathbf{u}_h = \mathbf{u}_e = \mathbf{0}$, then velocities and pose errors asymptotically converge to zero. That is

$$\lim_{t\to\infty} \dot{\mathbf{x}}_i(t) = \lim_{t\to\infty} \mathbf{e}_{ij}(t) = \mathbf{0} \qquad \square$$

Proof: Consider the following function

$$V_i = \frac{1}{2}\left[\dot{\mathbf{x}}_i^\top \mathbf{M}_i(\mathbf{q}_i)\dot{\mathbf{x}}_i + d_i|\dot{\mathbf{y}}_i|^2\right] + \delta_i \int_0^t \dot{\mathbf{x}}_i^\top(\sigma)\mathbf{u}^*(\sigma)d\sigma$$

where $\delta_\ell = -1$, $\delta_r = 1$, $\mathbf{u}^* = \mathbf{u}_h$ if $i = \ell$ and $\mathbf{u}^* = \mathbf{u}_e$ if $i = r$. From Assumption A1 and Property P1, it can be proved that V_i is positive semi-definite and radially unbounded with regards to $\dot{\mathbf{x}}_i$ and $\dot{\mathbf{y}}_i$. Its time–derivative, evaluated along (14) and using Property P2, yields

$$\dot{V}_i = -\dot{\mathbf{x}}_i^\top\left[k_i \mathbf{e}_{ij} + d_i \boldsymbol{\Psi}_i \dot{\mathbf{y}}_i\right] + d_i \dot{\mathbf{y}}_i^\top \ddot{\mathbf{y}}_i.$$

At this point one should note that

$$\begin{aligned} \dot{\mathbf{x}}_i^\top \boldsymbol{\Psi}_i \dot{\mathbf{y}}_i &= \mathbf{v}_i^\top \dot{\mathbf{y}}_{vi} + \frac{1}{2}\omega_i^\top \mathbf{U}^\top(\boldsymbol{\xi}_i)\dot{\mathbf{y}}_{\omega i} \\ &= \mathbf{v}_i^\top \dot{\mathbf{y}}_{vi} + \dot{\boldsymbol{\xi}}_i^\top \dot{\mathbf{y}}_{\omega i}, \end{aligned}$$

where (13) has been used to obtain the first equation and (8) for the second one. Further, using (11), the term $\dot{\mathbf{y}}_i^\top \ddot{\mathbf{y}}_i$ is

$$\dot{\mathbf{y}}_i^\top \ddot{\mathbf{y}}_i = -\dot{\mathbf{y}}_i^\top \mathbf{\Lambda}_i \dot{\mathbf{y}}_i + \dot{\mathbf{y}}_{vi}^\top \mathbf{v}_i + \dot{\mathbf{y}}_{\omega i}^\top \dot{\boldsymbol{\xi}}_i.$$

Using the previous equations yields $\dot{V}_i = -d_i \dot{\mathbf{y}}_i^\top \mathbf{\Lambda}_i \dot{\mathbf{y}}_i - k_i \dot{\mathbf{x}}_i^\top \mathbf{e}_{ij}$ which in view of (10) can be written as

$$\dot{V}_i = -d_i \dot{\mathbf{y}}_i^\top \mathbf{\Lambda}_i \dot{\mathbf{y}}_i - k_i \mathbf{v}_i^\top \tilde{\mathbf{p}}_{ij} - k_i \boldsymbol{\omega}_i^\top \tilde{\boldsymbol{\beta}}_{ij}.$$

Now, consider the error functional

$$W = \frac{1}{2} k_\ell |\tilde{\mathbf{p}}_{\ell r}|^2 + k_\ell \left[(1 - \tilde{\eta}_{\ell r})^2 + |\tilde{\boldsymbol{\beta}}_{\ell r}|^2 \right],$$

which is positive semi-definite and radially unbounded with regards to $\tilde{\mathbf{p}}_{\ell r}, 1 - \tilde{\eta}_{\ell r}$ and $\tilde{\boldsymbol{\beta}}_{\ell r}$. Its time–derivative yields

$$\begin{aligned} \dot{W} &= k_\ell \tilde{\mathbf{p}}_{\ell r}^\top \dot{\tilde{\mathbf{p}}}_{\ell r} - 2k_\ell (1 - \tilde{\eta}_{\ell r}) \dot{\tilde{\eta}}_{\ell r} + 2k_\ell \tilde{\boldsymbol{\beta}}_{\ell r}^\top \dot{\tilde{\boldsymbol{\beta}}}_{\ell r} \\ &= k_\ell \tilde{\mathbf{p}}_{\ell r}^\top \dot{\tilde{\mathbf{p}}}_{\ell r} + k_\ell \tilde{\boldsymbol{\beta}}_{\ell r}^\top \tilde{\boldsymbol{\omega}}_{\ell r} \end{aligned}$$

where, to obtain the second equation, (9) has been used together with the properties of the skew–symmetric matrices.

Defining $V = V_\ell + \frac{k_\ell}{k_r} V_r + W$ and using the fact that $\tilde{\mathbf{p}}_{ij} = -\tilde{\mathbf{p}}_{ji}$ and $\tilde{\boldsymbol{\beta}}_{ij} = -\tilde{\boldsymbol{\beta}}_{ji}$ yields

$$\dot{V} = -d_\ell \dot{\mathbf{y}}_\ell^\top \mathbf{\Lambda}_\ell \dot{\mathbf{y}}_\ell - \frac{d_i k_\ell}{k_r} \dot{\mathbf{y}}_r^\top \mathbf{\Lambda}_r \dot{\mathbf{y}}_r \leq 0.$$

Since $V \geq 0$ and $\dot{V} \leq 0$, $\dot{\mathbf{y}}_i \in \mathcal{L}_2$. Moreover, $\dot{\mathbf{x}}_i, \dot{\mathbf{y}}_i, \mathbf{e}_{\ell r} \in \mathcal{L}_\infty$ (since $\mathbf{e}_{\ell r} = -\mathbf{e}_{r\ell}$ then $\mathbf{e}_{r\ell} \in \mathcal{L}_\infty$). This finishes the first part of the proof.

For the second part, assume $\mathbf{u}_h = \mathbf{u}_e = \mathbf{0}$. In this case, the closed–loop system (14) becomes

$$\ddot{\mathbf{x}}_i = -\mathbf{M}_i^{-1}(\mathbf{q}_i) \left[\mathbf{C}_i(\mathbf{q}_i, \dot{\mathbf{q}}_i) \dot{\mathbf{x}}_i + k_i \mathbf{e}_{ij} + d_i \mathbf{\Psi}_i \dot{\mathbf{y}}_i \right].$$

From the above equation, note that if $\ddot{\mathbf{x}}_i, \dot{\mathbf{x}}_i$ and $\dot{\mathbf{y}}_i$ are asymptotically convergent to zero then this implies that $\mathbf{e}_{ij}$ also asymptotically converge to zero.

The time–derivative of system (11) is

$$\ddot{\mathbf{y}}_i = -\mathbf{\Lambda}_i \dot{\mathbf{y}}_i + \left[\begin{array}{c} \mathbf{v}_i \\ \dot{\boldsymbol{\xi}}_i \end{array} \right], \tag{15}$$

hence, boundedness of $\dot{\mathbf{x}}_i, \dot{\mathbf{y}}_i$ and the relation (8) between angular velocity and time–derivative of the quaternion ensure that $\ddot{\mathbf{y}}_i \in \mathcal{L}_\infty$. This last and $\dot{\mathbf{y}}_i \in \mathcal{L}_2$ supports the fact that $\lim_{t\to\infty} \dot{\mathbf{y}}_i(t) = \mathbf{0}$. Hence

$$\lim_{t\to\infty} \int_0^t \ddot{\mathbf{y}}_i(\sigma) d\sigma = \lim_{t\to\infty} \dot{\mathbf{y}}_i(t) - \dot{\mathbf{y}}_i(0) = -\dot{\mathbf{y}}_i(0).$$

Moreover, since $\ddot{\mathbf{y}}_i, \dot{\mathbf{y}}_i, \dot{\mathbf{x}}_i, \mathbf{e}_{ij} \in \mathcal{L}_\infty$, it can be easily proved —from the closed–loop system and the time–derivative of (15)— that $\ddot{\mathbf{x}}_i$, $\frac{d}{dt}\ddot{\mathbf{y}}_i \in \mathcal{L}_\infty$. This in turn, implies that $\ddot{\mathbf{y}}_i$ is uniformly continuous. A direct application of Barbalăt's Lemma ensures that $\lim_{t\to\infty} \ddot{\mathbf{y}}_i(t) = \mathbf{0}$ and from (15) that $\lim_{t\to\infty} \mathbf{v}_i(t) = \lim_{t\to\infty} \dot{\boldsymbol{\xi}}_i(t) = \mathbf{0}$, thus from (8), $\lim_{t\to\infty} \dot{\mathbf{x}}_i(t) = \mathbf{0}$.

Finally, convergence to zero of $\ddot{\mathbf{x}}_i$ is ensured by Barbalăt's Lemma with the facts that $\lim_{t\to\infty} \int_0^t \ddot{\mathbf{x}}_i(\sigma) d\sigma = -\dot{\mathbf{x}}_i(0)$ and that $\ddot{\mathbf{x}}_i$ is uniformly continuous. Hence $\lim_{t\to\infty} \mathbf{e}_{ij}(t) = \mathbf{0}$. This completes the proof. ∎

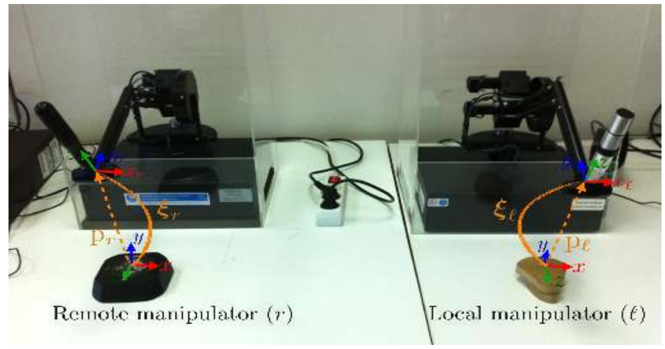

Fig. 2: Experimental validation setup.

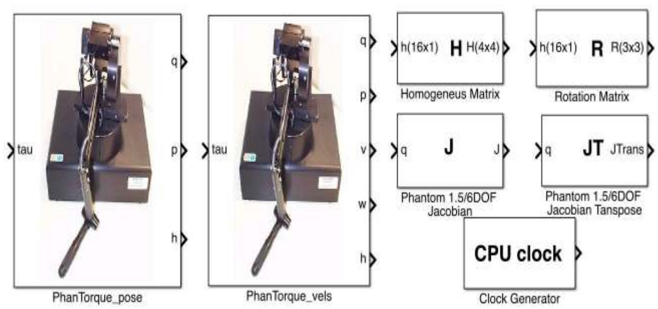

Fig. 3: PhanTorque library

IV. Experimental Validation

Fig. 2 depicts the experimental setup used for the validation. The local robot is a PHANTOM Premium 1.5® Haptic Device and the remote robot is a PHANTOM Premium 1.5 High Force® Haptic Device. Both robots have 6-DoF and are fully actuated (http://www.sensable.com). Each of the robots is connected to a computer through the parallel port, the controllers are programmed using Matlab version 7.11 and Simulink version 7.6. The communication channel, which transmits the pose from the local to the remote sites, and vice-versa, is implemented through UDP ports within the local laboratory network. The communications between the haptic devices and the computer is done using a Simulink library developed within this work, called *PhanTorque* (see Fig. 3). This library has been designed following the similar idea of the Phansim library in [26], the main differences between them is that the PhanTorque library allows to set the torques to the 6 haptic's actuators, and can read the position and the transformation matrix of the haptic's end-effector.

The gravitational torques vectors for the two robots, $\mathbf{g}_i(\mathbf{q}_i) \in \mathbb{R}^6$, have been approximated by calculating the gradient of the potential energy of the three haptic's segments (l_1, l_2, l_3), which are shown in Fig. 4. The gravity vector for both robots is defined by equation (16), where g is the gravity constant. The gravity vector parameters shown in the TABLE I have been estimated in the context of this work as an additional contribution. The Jacobian of the haptic devices can be found, in detail, in [27]. The controllers and the velocity estimator gains have been set to $k_\ell = 17$, $d_\ell = 1.5$, $k_r = 20$, $d_r = 7$, and $\mathbf{\Lambda}_i = 1000\mathbf{I_7}$.

$$\mathbf{g}_i(\mathbf{q}_i) = \begin{bmatrix} 0 \\ g((m_{1i}lc_{1i} + m_{2i}l_{1i} + m_{3i}l_{1i})\cos(q_{2i}) + (m_{2i}lc_{2i} + m_{3i}l_{2i})\sin(q_{3i}) + m_{3i}l_{3i}\cos(q_{3i} + q_{5i})) \\ g((m_{2i}lc_{2i} + m_{3i}l_{2i})\sin(q_{3i}) + m_{3i}lc_{3i}\cos(q_{3i} + q_{5i})) \\ g(m_{3i}lc_{3i}\sin(q_{3i} + q_{5i})sin(q_{4i})) \\ g(m_{3i}lc_{3i}\cos(q_{3i})\cos(q_{5i})) \\ 0 \end{bmatrix} \tag{16}$$

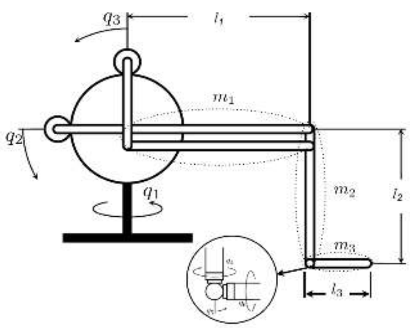

Fig. 4: Segments and masses of the robots.

Parameter	Local robot	Remote robot
Masses (kg)	m_1=0.0056 m_2=0.005 m_3=0.09	m_1=0.026 m_2=0.01 m_3=0.09
Lengths (m)	l_1=0.21 l_2=0.21 l_3=0.1	l_1=0.21 l_2=0.21 l_3=0.07
Center of masses (m)	lc_1=0.105 lc_2=0.21 lc_3=0.1	lc_1=0.105 lc_2=0.21 lc_3=0.07

TABLE I: Estimated parameters of the gravity vectors.

Fig. 5 and Fig. 6 show the pose time evolution of the local and the remote robots. During the first 1.5s, the gravity compensation term (16) is applied to both robots, which allows to set different initial conditions. At 1.5s, the proposed controllers (12) are activated and the local and the remote robots asymptotically converge to a common pose. From second 4 to second 22, a human operator exerts forces in the local manipulator end-effector. From these results we can conclude that the remote robots asymptotically tracks the local robot trajectory. Finally, when there are no external forces on the local and the remote robots, their pose converge again to a common pose (last three seconds). The pose error behavior is shown in Fig. 7. Fig. 8 and Fig. 9 present the experimental results for the linear and the angular velocities, respectively. In these figures it is observed that the errors and velocities asymptotically converge to zero after the controllers are activated, that the errors are bounded when external forces appear and that the pose error converges to zero when there are not any external force. These experimental results confirm the performance of the theoretical results reported in this work.

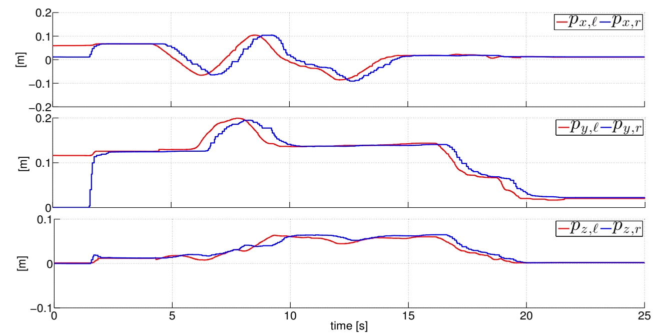

Fig. 5: Local and remote robots positions.

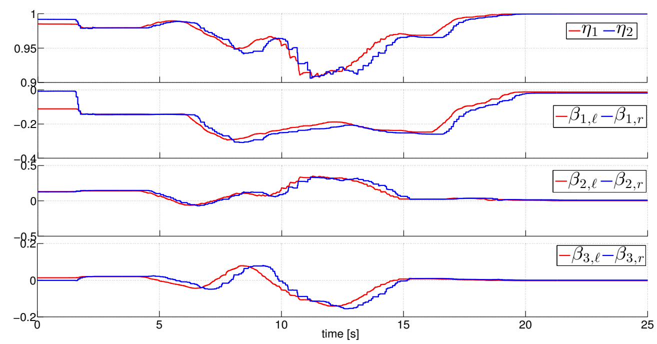

Fig. 6: Local and remote robots orientations.

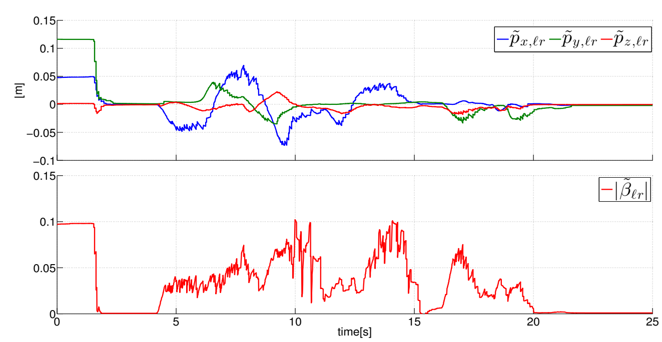

Fig. 7: Teleoperation system pose errors.

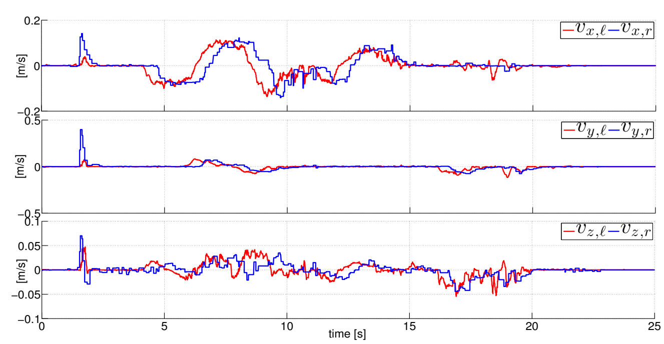

Fig. 8: Local and remote robots linear velocities.

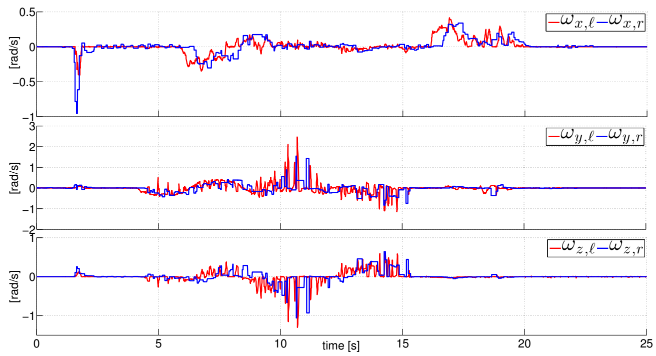

Fig. 9: Local and remote robots angular velocities.

V. Conclusions

This paper proposes a P + d controller, for a bilateral teleoperation system, which does not require the linear and the angular velocity measurements for its implementation. The controller has been designed in the operational space and it employs unit quaternions to describe the end-effectors' orientations. Unit quaternions provide a singularity-free orientation representation contrary to the minimal representations. Under a passivity assumption on the human operator and on the remote environment, boundedness of all signals has been established. Moreover, the paper also shows that, if the human operator and the environment do not exert forces on the manipulators, velocities and pose errors globally asymptotically converge to zero. The effectiveness of the proposed control scheme has been confirmed with experimental validation performed with two robots of 6-DoF.

A clear theoretical extension of the proposed scheme is the inclusion of time-delays in the communication channel. The fact that damping injection cannot be employed in the present scenario, due to the unavailability of velocity measurements, renders the authors' previous time-delay controllers [28], [29], [7] unsuitable for a possible extension. For this extension other Lyapunov–Krasovskiĭ or Lyapunov-Razumikhin functionals to prove stability with time-delays need to be found. However, we have systematically confirmed, in simulations and experiments, that the proposed schemes are robust to time-delays, but such assertion remains to be proven theoretically.

Acknowledgements

This work has been partially supported by: the Mexican CONACyT doctoral grant 168998; the Mexican projects CONACyT CB-129079 and the Spanish CICYT projects: DPI2010-15446 and DPI2011-22471.

References

[1] P. Hokayem and M. Spong. Bilateral teleoperation: An historical survey. *Automatica*, 42(12):2035–2057, 2006.
[2] E. Nuño, L. Basañez, and R. Ortega. Passivity-based control for bilateral teleoperation: A tutorial. *Automatica*, 47(3):485–495, 2011.
[3] R.J. Anderson and M.W. Spong. Bilateral control of teleoperators with time delay. *IEEE Trans. Autom. Control*, 34(5):494–501, 1989.
[4] G. Niemeyer and J.J. Slotine. Stable adaptive teleoperation. *IEEE J. Ocean. Eng.*, 16(1):152–162, 1991.
[5] S. Stramigioli, A. van der Schaft, B. Maschke, and C. Melchiorri. Geometric scattering in robotic telemanipulation. *IEEE Trans. Robot. Autom.*, 18(4):588–596, Aug. 2002.
[6] N. Chopra, M.W. Spong, R. Ortega, and N. Barbanov. On tracking preformance in bilateral teleoperation. *IEEE Trans. Robot.*, 22(4):844–847, Aug. 2006.
[7] E. Nuño, R. Ortega, and L. Basañez. An adaptive controller for nonlinear teleoperators. *Automatica*, 46(1):155–159, 2010.
[8] L.G. García-Valdovinos, V. Parra-Vega, and M.A. Arteaga. Observer-based sliding mode impedance control of bilateral teleoperation under constant unknown time delay. *Robot. Auton. Syst.*, 55(8):609–617, August 2007.
[9] C. Hua and X.P Liu. Teleoperation over the internet with/without velocity signal. *IEEE Trans. Instrum. Meas.*, 60(1):4–13, 2011.
[10] D. Lee and M.W. Spong. Bilateral teleoperation of multiple cooperative robots over delayed communication networks: Theory. *IEEE Int. Conf. Robot. Autom.*, pages 360–365, 2005.
[11] P. Malysz and S. Sirouspour. A Kinematic Control Framework for Single-Slave Asymmetric Teleoperation Systems. *IEEE Trans. Robot*, pages 1–17, 2011.
[12] C. Aldana, E. Nuño, and L. Basañez. Bilateral teleoperation of cooperative manipulators. In *IEEE Int. Conf. Robot. Auto.*, pages 4274 –4279, may 2012.
[13] Liu Y.C. and N. Chopra. Controlled synchronization of heterogeneous robotic manipulators in the task space. *Robotics, IEEE Transactions on*, 28(1):268 –275, feb. 2012.
[14] J.S. Yuan. Closed-loop manipulator control using quaternion feedback. *IEEE Robot. Autom.*, 4(4):434–440, 1988.
[15] J.T.-Y. Wen and K. Kreutz-Delgado. The attitude control problem. *IEEE Trans. Autom. Control*, 36(10):1148–1162, 1991.
[16] O.E. Fjellstad. *Control of unmanned underwater vehicles in six degrees of freedom: a quaternion feedback approach*. PhD thesis, Norwegian Institute of Technology, University of Trondheim, 1994.
[17] F. Caccavale, P. Chiacchio, and S. Chiaverini. Task-space regulation of cooperative manipulators. *Automatica*, 36(6):879–887, June 2000.
[18] H. Wang and Y. Xie. Passivity based task-space bilateral teleoperation with time delays. In *IEEE Int. Conf. Robot. Auto.*, pages 2098–2103, 2011.
[19] F. Caccavale, B. Siciliano, and L. Villani. The role of euler parameters in robot control. *Asian Journal of Control*, 1(1):25–34, 1999.
[20] E. Nuño, L. Basañez, G. Obregón, and G. Solis. Bilateral teleoperation control without velocity measurements. *IFAC World Congress*, pages 332–337, 2011.
[21] M.W. Spong, S. Hutchinson, and M. Vidyasagar. *Robot Modeling and Control*. Wiley, 2005.
[22] R. Kelly, V. Santibáñez, and A. Loria. *Control of robot manipulators in joint space*. Springer-Verlag, 2005.
[23] J.C.K. Chou. Quaternion kinematic and dynamic differential equations. *IEEE Trans. Robot. Autom.*, 8(1):53–64, 1992.
[24] J. B. Kuipers. *Quaternions and Rotation Sequences: A Primer with Applications to Orbits, Aerospace and Virtual Reality*. Princeton University Press, 2002.
[25] R. Campa and K. Camarillo. Unit quaternions: A mathematical tool for modeling, path planning and control of robot manipulators. *Robot manipulators, M. Ceccarelli (ed.), In-Teh*, pages 21–48, 2008.
[26] A Mohammadi, M Tavakoli, and A Jazayeri. Phansim : A Simulink Toolkit for the Phantom Haptic Devices. *Proc. of 23rd Canadian Congress of Applied Mechanics*, pages 787–790.
[27] A. Rodríguez and L. Basañez. Modelo cinemático de la interfase háptica phantom 1.5/6dof. technical university of catalonia (http://upcommons.upc.edu/pfc/handle/2099.1/14587). 2005.
[28] E. Nuño, R. Ortega, N. Barabanov, and L. Basañez. A globally stable PD controller for bilateral teleoperators. *IEEE Trans. Robot.*, 24(3):753–758, June 2008.
[29] E. Nuño, L. Basañez, R. Ortega, and M.W. Spong. Position tracking for nonlinear teleoperators with variable time-delay. *Int. J. Robot. Res.*, 28(7):895–910, July 2009.